LOOP DETECTOR SAMPLING FREQUENCY ERRORS AFFECTING LENGTH BASED CLASSIFICATIONS

A Thesis

Presented in Partial Fulfillment of the Requirements for Graduations *with distinction* in Civil Engineering with the Bachelor of Science Degree from the College of Engineering at The Ohio State University

By: Troy A. Karski

*****

The Ohio State University

2012

Thesis Review Committee:

Dr. Benjamin Coifman, Advisor

Abstract

The classification of vehicles has multiple purposes, including, but not limited to, roadway planning, quantifying environmental impacts, and determining roadway deterioration. Length based classifications from loop detectors is a common way to classify the vehicles, where a loop detector is effectively a metal detector embedded in the pavement that can measure when a vehicle is over the loop. Loop detectors can operate from 60 Hz to over 1000 Hz. As this work demonstrates, when a loop detector is operating at a lower frequency, the sampling resolution can lead to large errors due to the large, discrete steps between observable measurements.

This problem has been elusive since large quantities of ground truth speeds and lengths for vehicles are prohibitively difficult to collect. To bypass this problem a simulation model is developed to calculate the length measurement errors arising from a given detector's sampling period. The derivation of the sampling error can explain some of the length errors seen in vehicle classification. Finally, to empirically validate the model, this work uses a low sampling frequency LIDAR sensor (40 Hz) that is deployed concurrent with a conventional loop detector based classification station (300 Hz). The 40 Hz data are evaluated in the context of the 300 Hz data, since the relative impact of the sampling errors should be very small in the latter case. However, an additional complication arose because the spacing between detectors differs and introduces a secondary source of errors. As such, the LIDAR data analysis was inconclusive.

This Page Intentionally Left Blank

Acknowledgements

I would like to thank Dr. Benjamin Coifman for his continued work advising this research over the past year. His knowledge and dedication were vital to ensuring the success of this project.

I would also like to the Ho Lee, whose skill with statistics, allowed conclusions to be drawn from the data, also for his help in locating loop detector and LIDAR data, without which, much of my analysis would not have been possible. My sincere thanks to the College of Engineering at The Ohio State University for their generous financial support, which allowed me to devote time to research as an undergraduate.

Also, I would like to thank Seoungbum Kim, who calculated sampling rates of loop detectors, which was vital to my research.

Finally, I thank my parents, who have taught me to persevere and work hard, and who continue to support me throughout all of my endeavors.

Table of Contents

List of Figures

Introduction

Each state's department of transportation monitors the flow of vehicles. These vehicles are often classified by vehicle type or classification. These classifications are used for roadway planning, quantifying environmental impacts, or determining road deterioration. Perhaps the simplest way to classify vehicles is by length based classification. Length based classification is the process of putting a vehicle into a group based on its length. The Ohio Department of Transportation separates the vehicles into three classification groups: *0 to 28 feet*, *28 to 46 feet*, and *longer than 46 feet*. These groups are meant to represent passenger cars, single unit trucks and dual unit trucks, respectively [1].

A common way to determine the length of a vehicle is to use loop detectors, where a loop detector is effectively a metal detector embedded in the pavement that can measure when a vehicle is over the loop. Single loop detectors have just one loop per lane, as a result, it is impossible to separate the impacts of a given vehicle's speed from those of its length. Dual loop detectors have two loops detectors per lane, allowing for direct measurement of traversal time (and thus speed) between the paired loops, which then allows for direct vehicle length calculation. Typically loop detectors have sampling periods that range from 60 Hz to over 1000 Hz. Although conventional practice ignores the impacts of the discrete sampling periods, this work shows that the discretization can create an error in the dual loop detector based speed and length measurements. If the vehicle is within a few feet of the boundary between two length bins, a length error can also cause the vehicle to be misclassified.

Loop Detector Errors

Sampling error is caused by the rate at which the loop detector samples. For example a common sampling rate is 60 Hz, or 60 times a second. Since the loop detector is not measuring data in continuous time, the speed and length will exhibit small errors due to the discretization. These sampling errors have conventionally been assumed to be negligible, though as noted above, the errors can sometimes be large enough to result in misclassifications. Furthermore, dual loop detectors cannot easily measure acceleration. This study follows conventional practice for calculating the speed of a given vehicle whereby the acceleration is assumed to be negligible. This assumption is reasonable at free flow speeds, but breaks down at slower speeds, e.g., stop-and-go traffic. To avoid the confounding impacts of acceleration, induced errors, this study uses strictly free flow traffic conditions.

Theory

A dual loop detector measures four events as a vehicle passes, denoted $\text{on}_1, \text{off}_1, \text{on}_2,$ and off_2 in figure 1 (B). Using these four times, dual loop detectors can measure the elapsed time for the vehicle to cross the first and second detector, or traversal time (TT), either on_2-on_1 or off_2-off_1. Speed, v, can then be calculated from the quotient of the known detector spacing and TT (Equation 1). The vehicle will be on the loop detector for a measured amount of time, or on-time (OnT), either off_1-on_1 or off_2-on_2. The effective vehicle length is the product of speed and OnT (Equation 2). Since length is a function of speed, the error in length will be caused by the on-time and traversal time. Note, as evident in figure 1 (A), effective vehicle length differs from the actual vehicle length because the effective vehicle length includes the length of the detector.

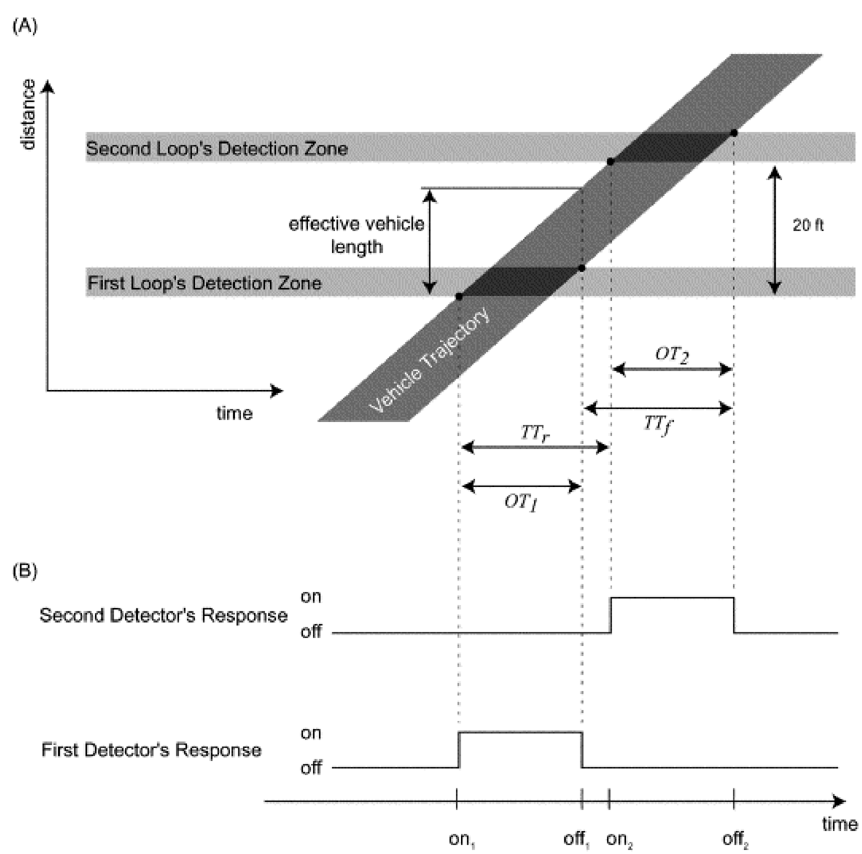

Figure 1: The pulse a vehicle makes over a dual loop detector (from [4])

$$v = \frac{distance\ between\ loops}{TT} \tag{1}$$

$$L = (OnT) * v \tag{2}$$

$$L = \frac{(OnT) * distance\ between\ loops}{TT} \tag{3}$$

While Figure 1 (B) shows the measurements in continuous time, in reality the controller samples the detectors at discrete intervals. Since the loop detectors do not sample in a continuous manor, there will likely be sub-sample-period errors in the measured rising edge time and the measured falling edge time. These errors will create OnT and TT errors which will cause errors in the v and L measurements from Equations 1-3. Figure 2 repeats the same vehicle's pulses over the dual loop detector, the dashed line indicates the true pulse in continuous time and the solid line indicates the measured pulse in discrete time (note that in this figure the upstream and downstream pulse are shown on the same axis). Henceforth, ϵ_r and ϵ_f are used to denote the difference in actual time of a transition (in continuous time) and the recorded time (discretized by the controller). The measurement resolution is only as precise as the sample period, T, as shown by tick marks along the time axis in Figure 2. A given event will have happened between 0 and T prior to the recorded time, and this error can be observed at each of the rising and falling edges in the figure. The maximum sampling error for any one event should be one sampling period. Thus, the range of error due to discretization for OnT and TT is +/-T.

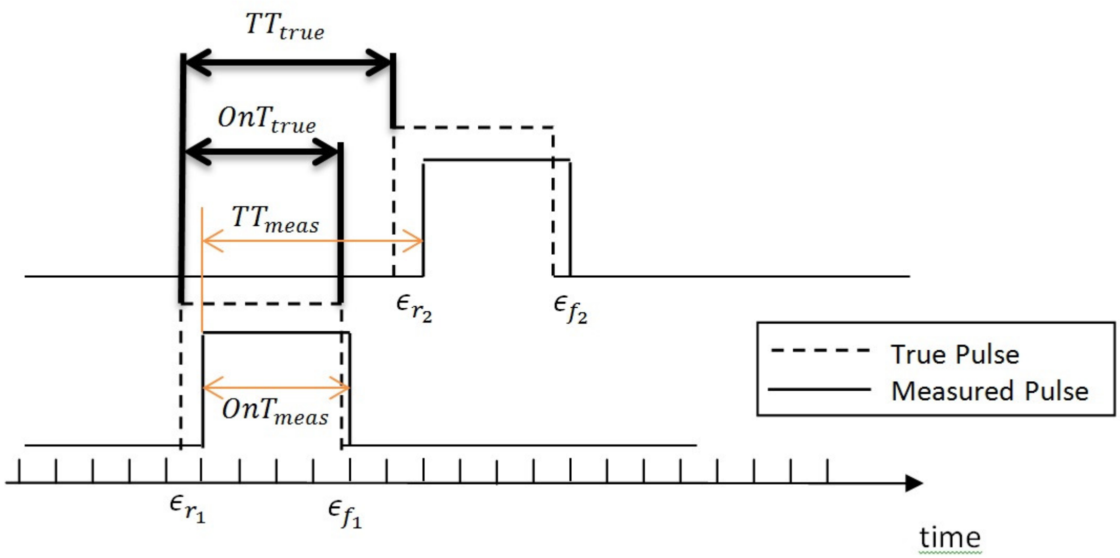

Figure 2: The pulses of a vehicle going over a dual loop detector, both in continuous time and the discrete measurements

$$TT_{true} = t_{r_2} - t_{r_1} \quad (4)$$

$$OnT_{true} = t_{f_1} - t_{r_1} \quad (5)$$

Where t_{r_x} is on_x and t_{f_x} is off_x.

Without loss of generality, this study uses OT_1 and TT_R (Figure 1 (A)) and the corresponding continuous measurements from Equations 4-5. For the simulation model the measured OnT and TT will each have two random errors, denoted ϵ_{x_n}, uniformly distributed between 0 and T. Equation 6 and 7 show the calculation of measured traversal time and on-time.

$$TT_{meas} = t_{r_2} - t_{r_1} - \epsilon_{r_1} + \epsilon_{r_2} = TT_{true} - \epsilon_{r_1} + \epsilon_{r_2} \quad (6)$$

$$OnT_{meas} = t_{f_1} - t_{r_1} - \epsilon_{r_1} + \epsilon_{f_1} = OnT_{true} - \epsilon_{r_1} + \epsilon_{f_1} \quad (7)$$

In other words, the measured TT is just the sum of the true traversal time and the error in TT. Similarly, the measured OnT is the sum of the true OnT and the error. Equations 8-9 show how these errors translate to the L and V measurements.

$$v_{meas} = \frac{distance\ between\ loops}{TT_{meas}} = \frac{distance\ between\ loops}{TT_{true} - \epsilon_{r_1} + \epsilon_{r_2}} \quad (8)$$

$$L_{meas} = (OnT_{meas}) * v_{meas} = \left(OnT_{true} - \epsilon_{r_1} + \epsilon_{f_1}\right) * v_{meas} \quad (9)$$

The OnT error is calculated by taking the falling edge error from the first loop detector and subtracting it by the rising edge error of the first loop detector. The TT error is calculated by taking the second detector's rising edge error and subtracting it by the first loop detector's rising edge error. The rising and falling edge errors for all of the transitions are defined to be strictly positive even though they represent a negative time. Thus, because of the addition and subtraction, the distributions for both OnT and TT are between –T and T. When looking at many vehicles, the errors for each transition event are sampled from a uniform distribution. The sum of two independent uniformly distributed random variables creates a density function that looks triangular [2]. In this case the transitions do have some dependence (the paired loop detectors are on a common clock cycle, while the vehicle is of a fixed length and travels at a fixed speed), but the impact is small. Figure 3 and 4 below show the distribution of the on-time error, the traversal time error and the combined traversal time versus on-time error for 100,000 samples. These figures are plotted as a percentage of the sampling period. Figure 5 shows how the distribution would be if the first loop detector was used to determine the on-time and the traversal time was determined by using the rising edges. Figure 6 is the distribution of the on-time and traversal time errors using the second loop and rising edges respectively. Note from the scatter plots in these figures that OnT and TT errors are correlated since they share a common event.

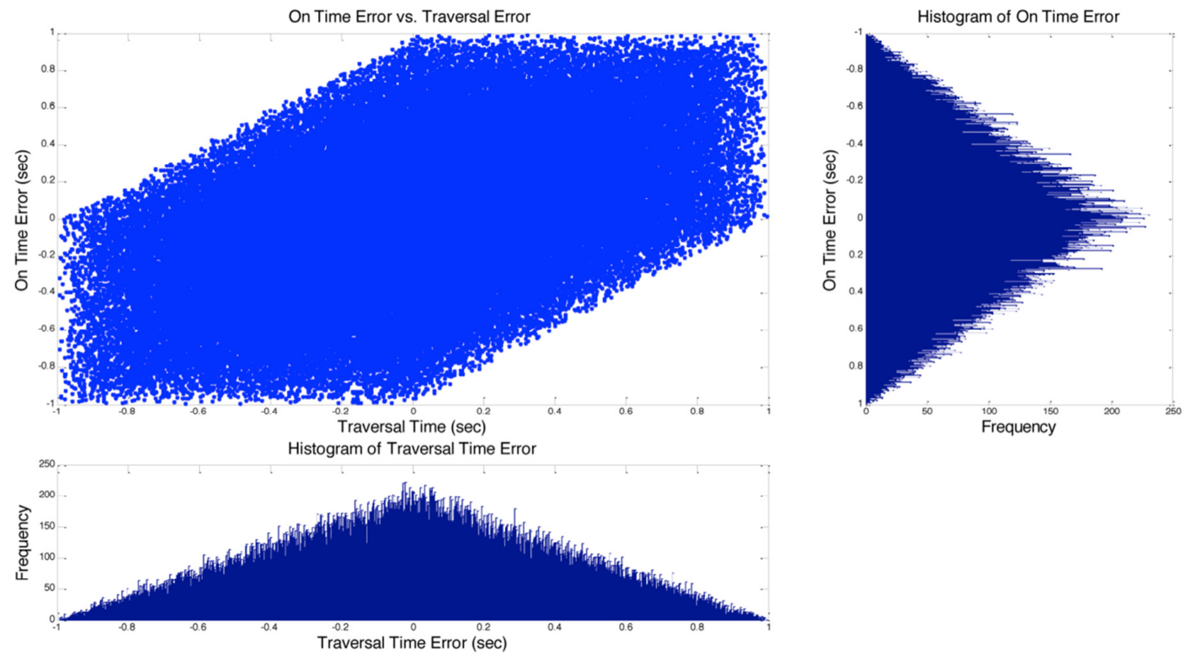

Figure 3: Distribution of on-time and traversal time errors using the first loop and rising edges

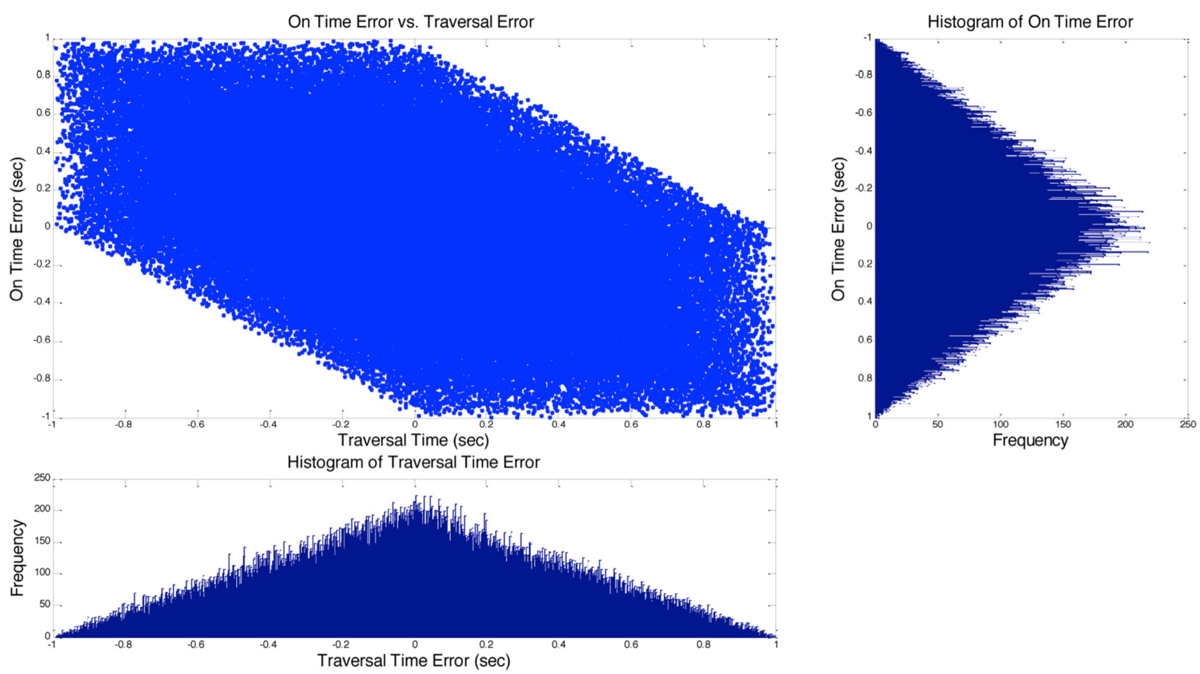

Figure 4: Distribution of on-time and traversal time errors using the second loop and rising edges

The speed and length errors are calculated from equations 10 and 11, respectively. The results of the calculations represent the deviation between the measured and actual speeds and lengths. The error can be positive or negative due to the distribution of the on-time error and traversal time error, which makes the true speed or length larger or smaller than the measured speed or length.

$$V_{error} = V_{true} - V_{meas} \tag{10}$$

$$L_{error} = L_{true} - L_{meas} \tag{11}$$

Methodology

Due to the inherent difficulty of collecting empirical ground truth data, a simulation model is developed and used in this study. The Monte Carlo method was used to simulate vehicles traveling over a dual loop detector. Given a measured length and speed, the true length and speed can be simulated. To ensure that the traversal time chosen would give a vehicle in free flow speed, the speed was chosen and the traversal time was calculated. The focus of this study is ultimately the impact on length based vehicle classification, and the closer a length is to the boundary between two bins, the more likely that a small length measurement error could result in a misclassification. As such, this study considers the *worst case* scenario, a vehicle length exactly equal to the boundary between length bins, either 28 or 46 feet. The resulting distribution of length errors can also be used to estimate the range of lengths that are vulnerable to being misclassified due to the length measurement error. Since the true velocity and length are assigned by the simulation, TT_{true} and OnT_{true} are constant, and the resulting errors can be calculated from Equations 8-11 by randomly selecting ϵ_{r_1}, ϵ_{r_2}, ϵ_{f_1}, and ϵ_{f_2}..

Figures 5-7 show the distribution of speed and length errors for different detector sampling frequencies. The frequencies chosen are 40 Hz, 60 Hz, and 300 Hz. Figure 8, shows the cumulative distribution of all three frequencies for length and speed errors.

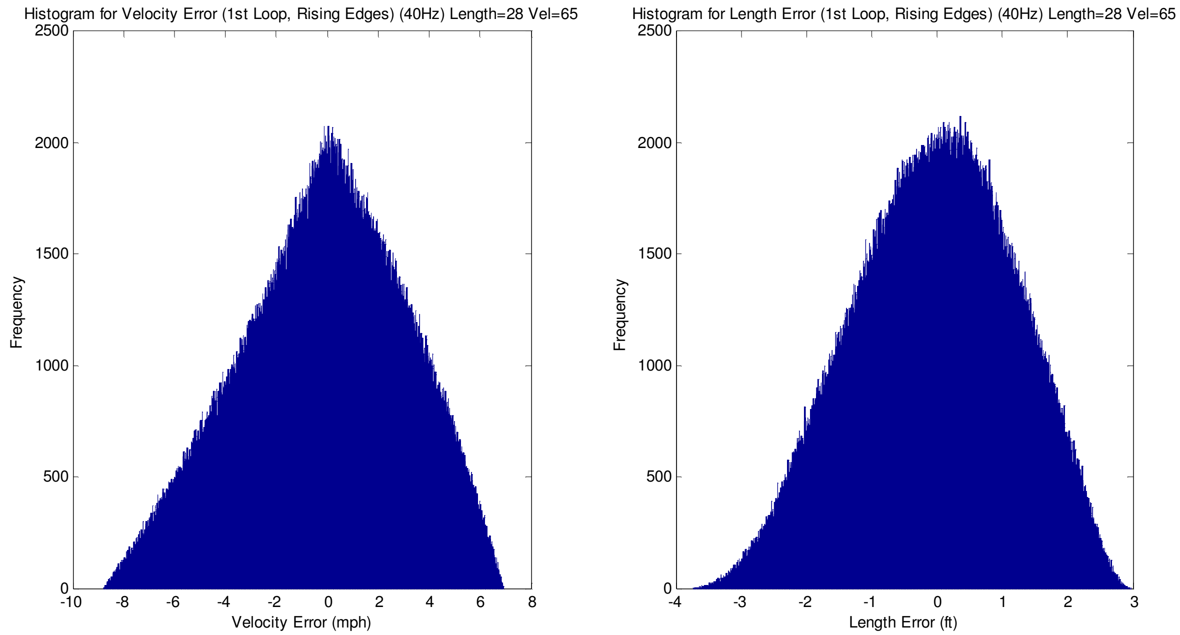

Figure 5: Histogram of speed error and length error for 100,000 simulated vehicles at 40 Hz

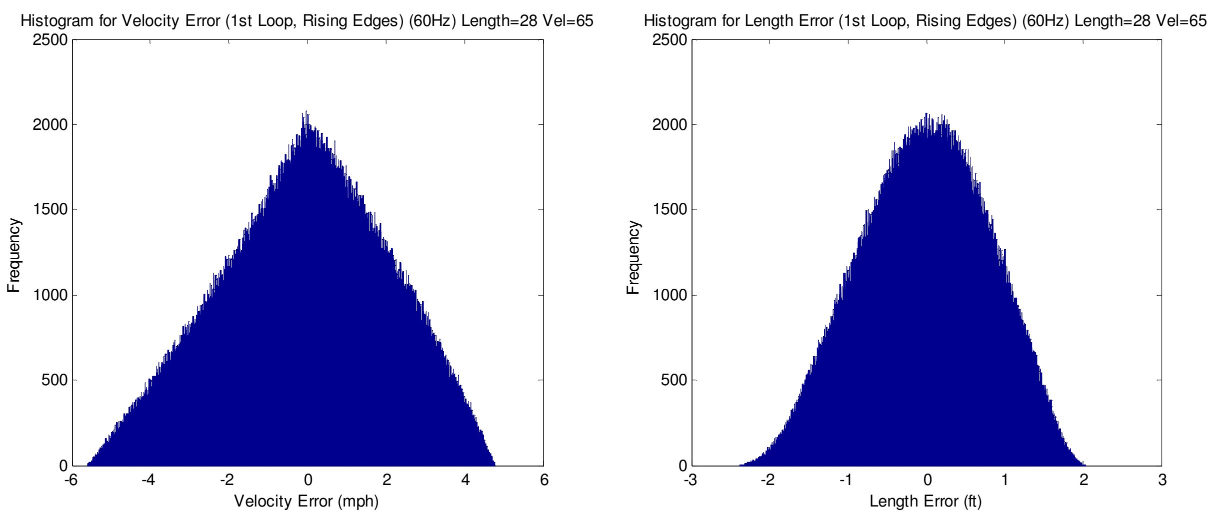

Figure 6: Histogram of speed error and length error for 100,000 simulated vehicles at 60 Hz

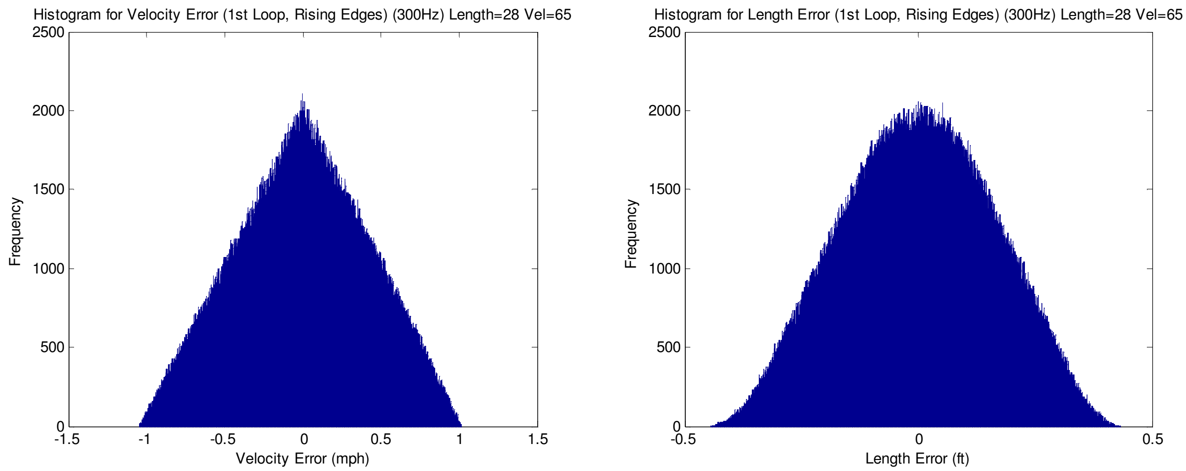

Figure 7: Histogram of speed error and length error for 100,000 simulated vehicles at 300 Hz

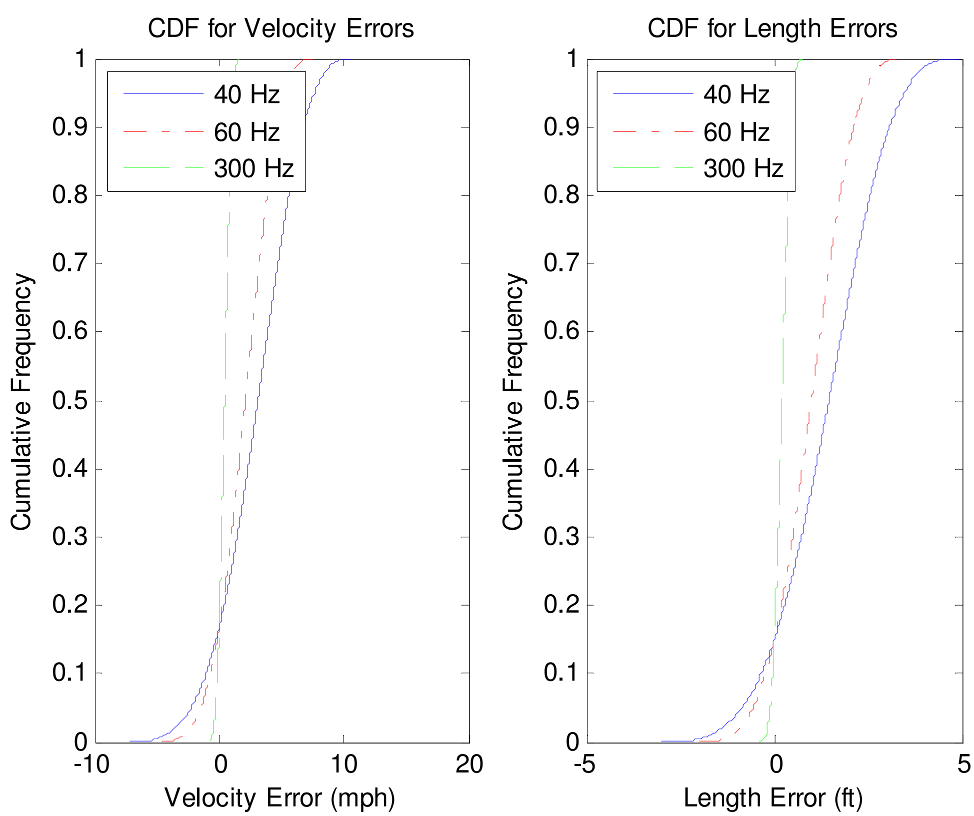

Figure 8: Cumulative distribution function for speed and length errors at 40, 60, and 300 Hz

Although some of the plots may seem symmetric, because the traversal time error impacts the denominator, it creates an asymmetrical distribution. This problem becomes more apparent when the sampling frequency is smaller or the distance between the detectors becomes smaller.

Due to equation 9, the true length of a vehicle will impact the range of possible length error. Larger vehicles will have a larger possible error since these larger vehicles have longer on-times. When on-times are larger, the multiplication of the on-time creates larger errors. Ultimately the present work is interested in vehicle classification. If a vehicle length is far from the boundaries between bins, even a large length measurement error will not result in a misclassification. Closer to the boundaries, however, a small length measurement error can result in a misclassification. As such, this study explicitly examines the errors for vehicle lengths at the boundaries, 28 ft and 46 ft. Figure 9 below compares the cumulative distribution function for vehicles with lengths of 28 feet and 46 feet traveling at 65 mph. These detectors are measuring at 40 Hz, and are 20 feet apart. The length does not affect the speed error; however, the reverse is not true. Since length is determined by the speed, when speed increases, the length error will increase. The error due to speed changes is seen in figure 10 using vehicle lengths of 28 feet, distance between loops 20 feet, and the detector operating at 40 Hz.

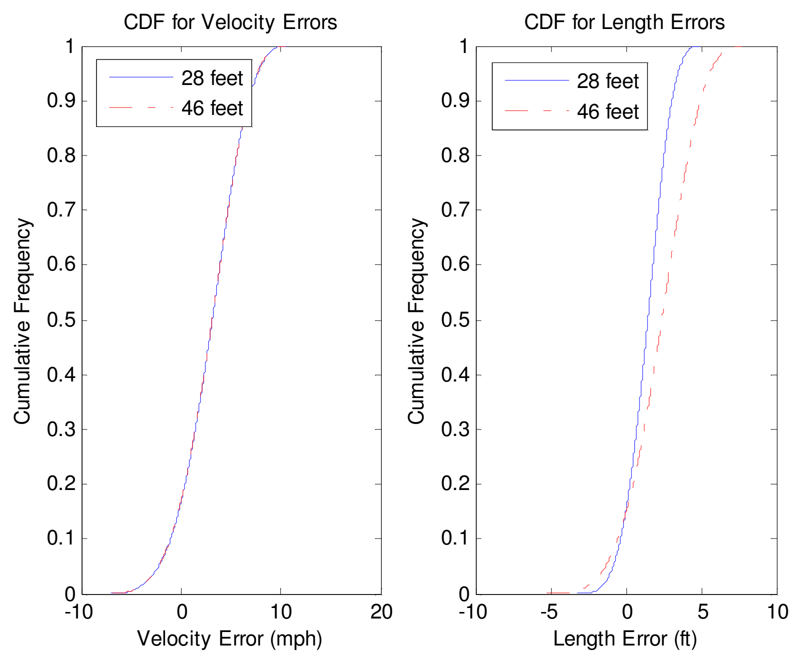

Figure 9: Cumulative distribution functions for vehicle lengths of 28 and 46 feet with 20 feet between the two detectors and sampling at 40 Hz.

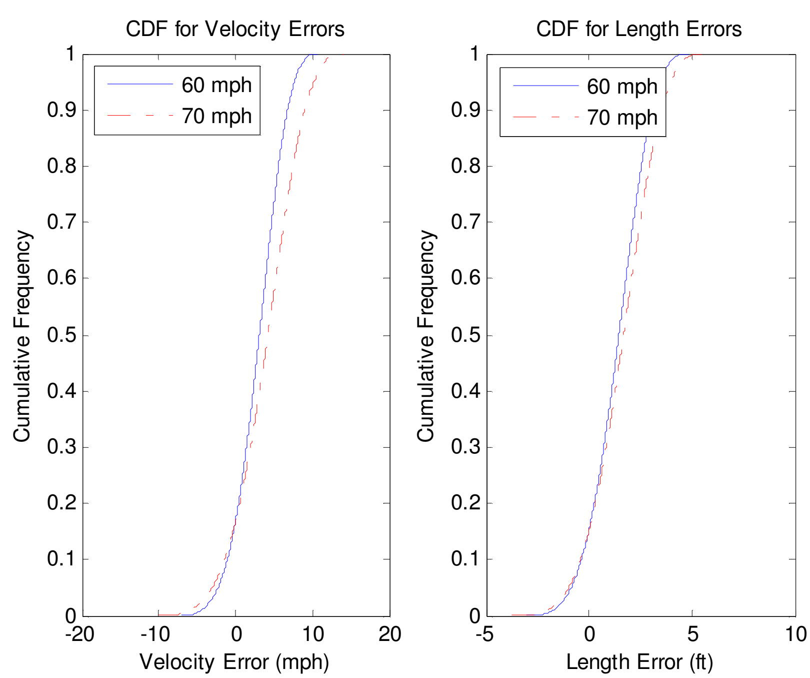

Figure 10: Cumulative distribution functions for vehicle speeds of 60 and 70 mph with 20 feet between the two detectors and sampling at 40 Hz.

Distance between Detectors Affecting Error

As seen previously in equation 1, the distance between detectors plays an important role in determining the speed of the vehicle. Normally, the traversal time would be measured, which would be used to calculate speed from equation 8-10, yielding Equations 12-13,

$$V_{error} = \frac{\left(V_{true} * \left(\frac{dist}{V_{true}} - \epsilon_{r_1} + \epsilon_{r_2}\right)\right) - (dist)}{\frac{dist}{V_{true}} - \epsilon_{r_1} + \epsilon_{r_2}} \tag{12}$$

Simplifying,

$$V_{error} = \frac{(V_{true} * \epsilon_{r_2} - V_{true} * \epsilon_{r_1})}{\frac{dist}{V_{true}} - \epsilon_{r_1} + \epsilon_{r_2}} \tag{13}$$

Thus, as the distance between loops increases, the speed error will decrease (assuming acceleration is negligible, which is a reasonable assumption at free flow speeds).

The example below demonstrates the impact of detector spacing, first for detectors separated 20 feet and then repeating the analysis for detectors separated by 5 feet. In both cases the detectors are sampled at 40 Hz.

$$V_{meas} = 60\ mph = 88\ ft/s$$

and suppose the individual transition time errors in this case happened to be:

$$\epsilon_{r_1} = 0.00625\ sec;\ \epsilon_{r_2} = 0.015\ sec$$

First, examine the impact of the detector separation of the detectors at 20 feet.

$$V_{error} = \frac{(88 * 0.015 - 88 * 0.00625)}{\frac{20}{88} - 0.00625 + 0.015} \approx 3.26 \frac{ft}{s} = 2.2\ mph$$

Then repeat when the detector separation is 5 feet:

$$V_{error} = \frac{(88 * 0.015 - 88 * 0.00625)}{\frac{5}{88} - 0.00625 + 0.015} \approx 11.74 \frac{ft}{s} = 8.0\ mph$$

Since the measured length is proportional to speed, the length errors will show a similar distribution. Figure 11 and 12 below, demonstrates the speed error and length error distributions respectively, when the distance between loops is 20 feet and 4.6 feet for a sampling rate of 40 Hz. The true length and speed of the vehicle is 20 feet and 65 mph, respectively. The absolute speed error can be as much as 70 mph when the distance between detectors is only 4.6 feet while this limit drops to 9 mph when the spacing is 20 feet. Similarly, the maximum absolute length error is 20 feet and 2.5 feet for detector spacing of 4.6 feet and 20 feet, respectively.[1]

[1] Note that conventional loop detectors are 6 feet, so the 4.6 foot spacing is infeasible for the loop detectors. We chose this small spacing to represent the LIDAR detectors used in the last portion of this study and which have a negligibly wide detection zone.

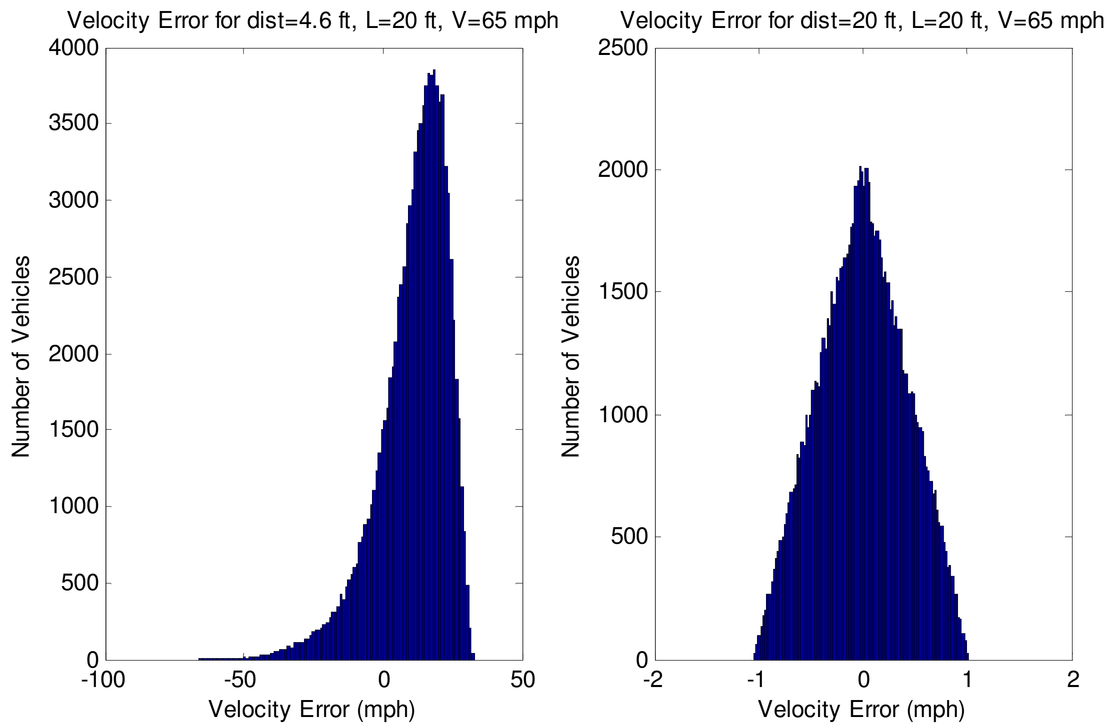

Figure 11: Histogram of speed error for 100,000 simulated vehicles at 40 Hz, using two different detector spacings.

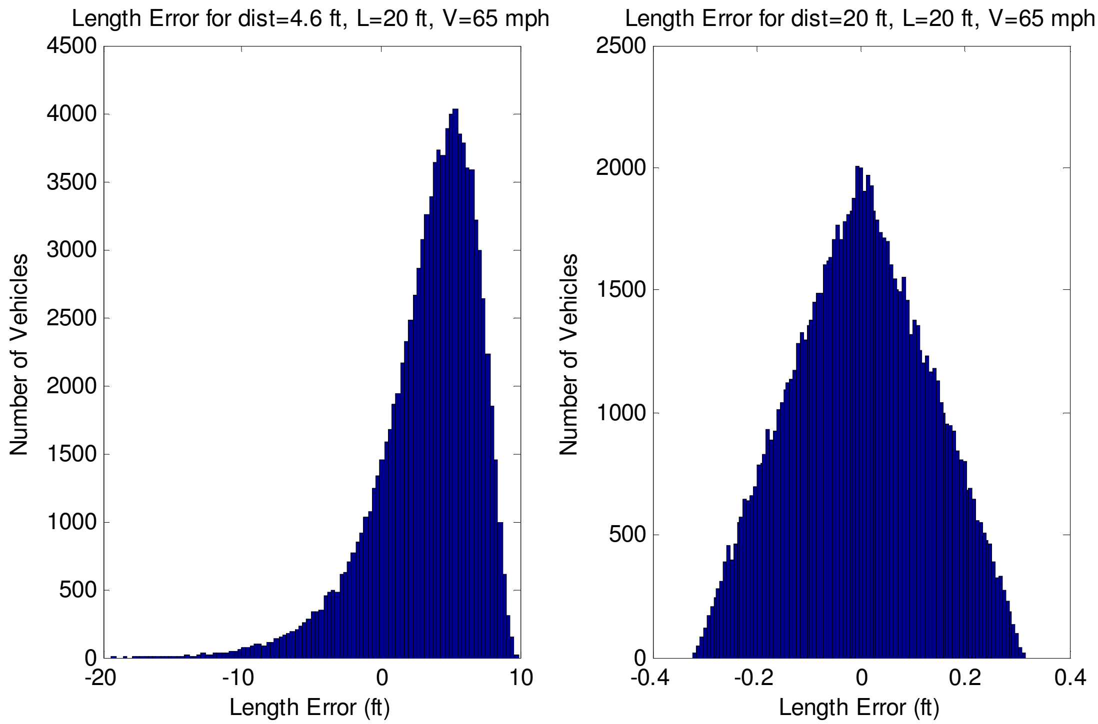

Figure 12: Histogram of length error for 100,000 simulated vehicles at 40 Hz, using two different detector spacings.

Figure 13 shows the cumulative distribution function for the speed and length errors of loop detector spacings of 4.6 and 20 feet. These plots show the larger absolute errors due to smaller detector spacing.

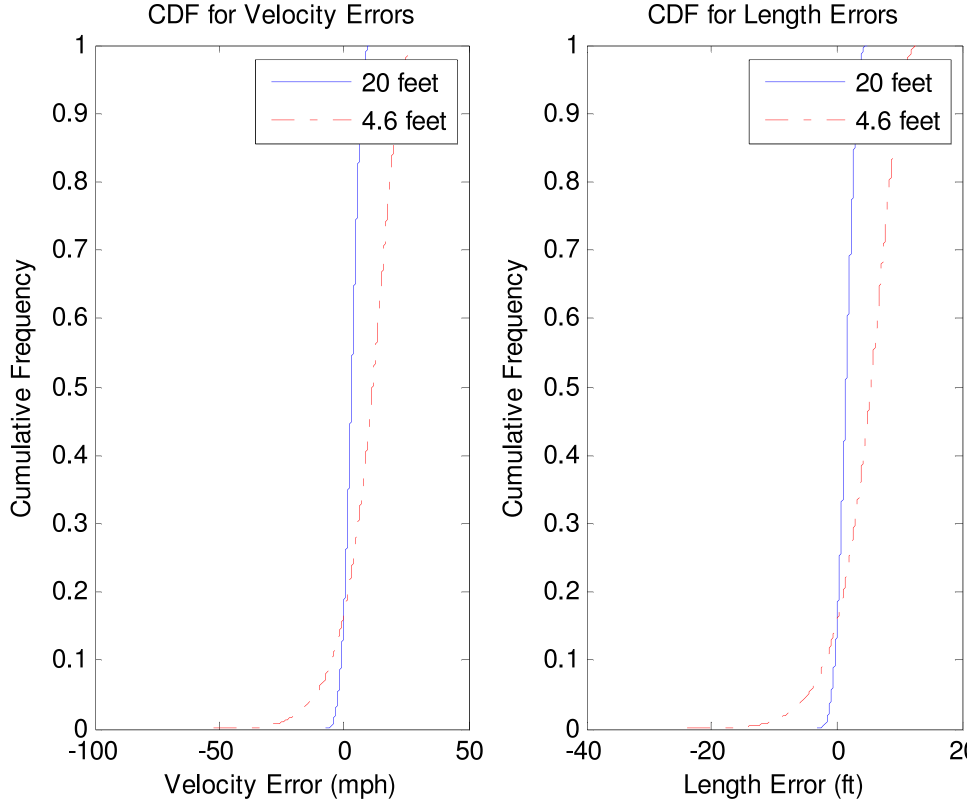

Figure 13: Cumulative Distribution function of speed and length errors for simulated vehicles at 40 Hz, using two different detector spacings.

Testing the Model with LIDAR

It is prohibitively labor intensive to collect accurate ground truth length and speed measurements. So in order to empirically evaluate the model against real world data, this work uses a LIDAR sensor with a relatively low sampling frequency (40 Hz) that is deployed concurrent with a conventional loop detector based classification station (300 Hz) on I-270 in Columbus, Ohio [3] for four hours. The 40 Hz data are evaluated in the context of the 300 Hz data. Since the relative impact of the sampling errors should be very small in the latter case, it is used as ground truth for the former case. However, as will be discussed, an additional complication arose because the spacing between detectors differs- LIDAR at 4.6 feet and dual loop detectors at 20 feet- which introduces a secondary source of errors. The paired LIDAR sensors were mounted on a van and Figure 14 shows the set up for the classification station for one lane.

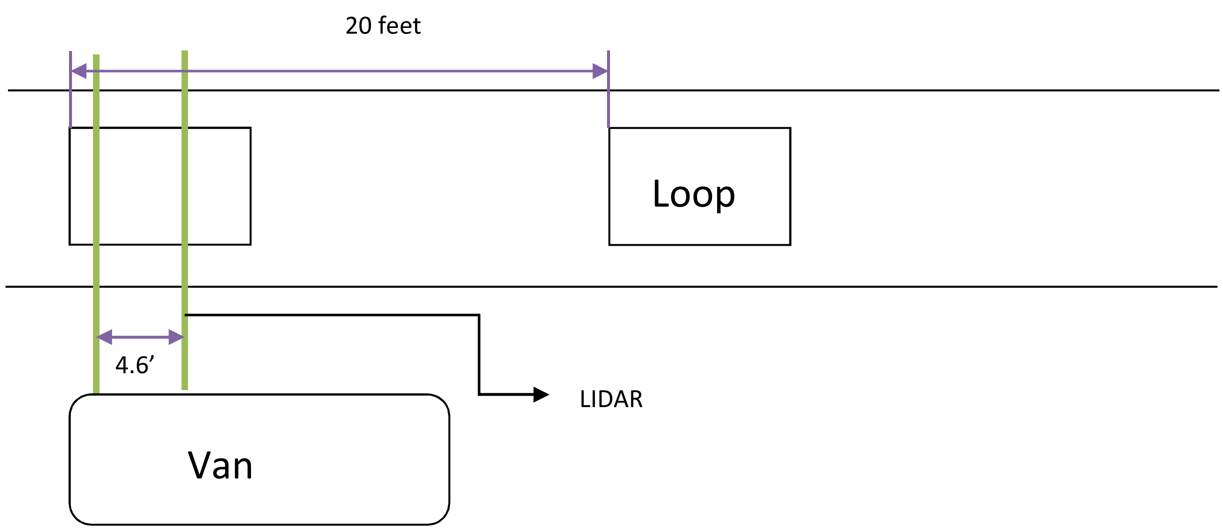

Figure 14: I-270 Classification station configuration

The LIDAR system used in this study does not have synchronized detectors, which introduces another error that can be up to one full sampling period, denoted as *shift* and modeled with another uniform distribution. The asynchronous detection changes the speed error because the traversal time would have an extra error in it. From equation 19:

$$V_{error} = \frac{\left(V_{meas} * \left(\frac{dist}{V_{meas}} + \epsilon_{r_1} - \epsilon_{r_2} + shift\right)\right) - (dist)}{\frac{dist}{V_{meas}} + \epsilon_{r_1} - \epsilon_{r_2} + shift}$$

When simplified becomes:

$$V_{error} = \frac{(V_{meas}*\epsilon_{r_1} - V_{meas}*\epsilon_{r_2} + V_{meas}*shift)}{\frac{dist}{V_{meas}} + \epsilon_{r_1} - \epsilon_{r_2} + shift} \quad (14)$$

From the equation above, the speed and length error distributions will change because of the shift. The resulting distributions are presented in figures 15 and 16 below assuming a true length of 20 feet, a true speed of 65 mph, and the distance between detectors of 4.6 feet.

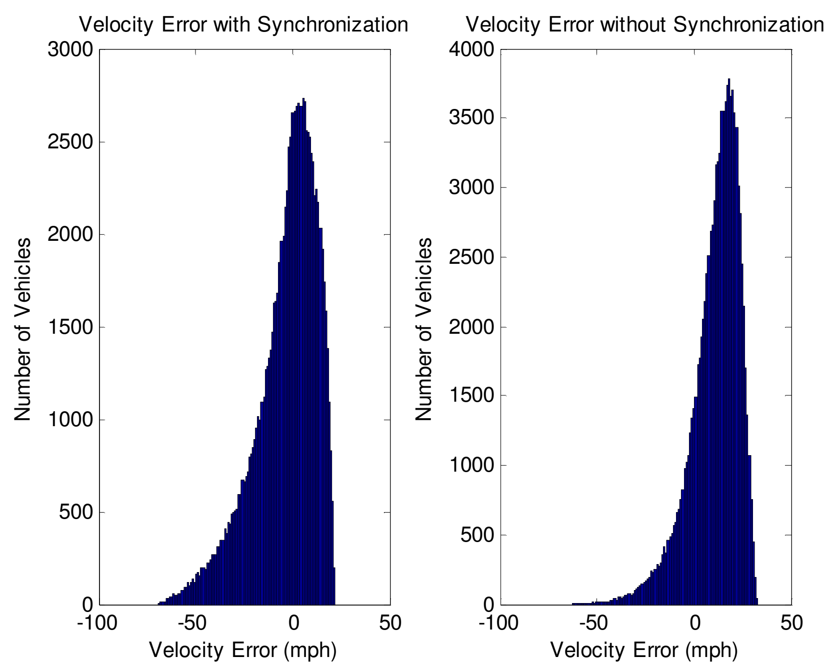

Figure 15: The effects of synchronous clocks on speed error: with synchronization on the left and without on the right. Note that in this case the effective range is smaller and shifts to the right for the asynchronous data.

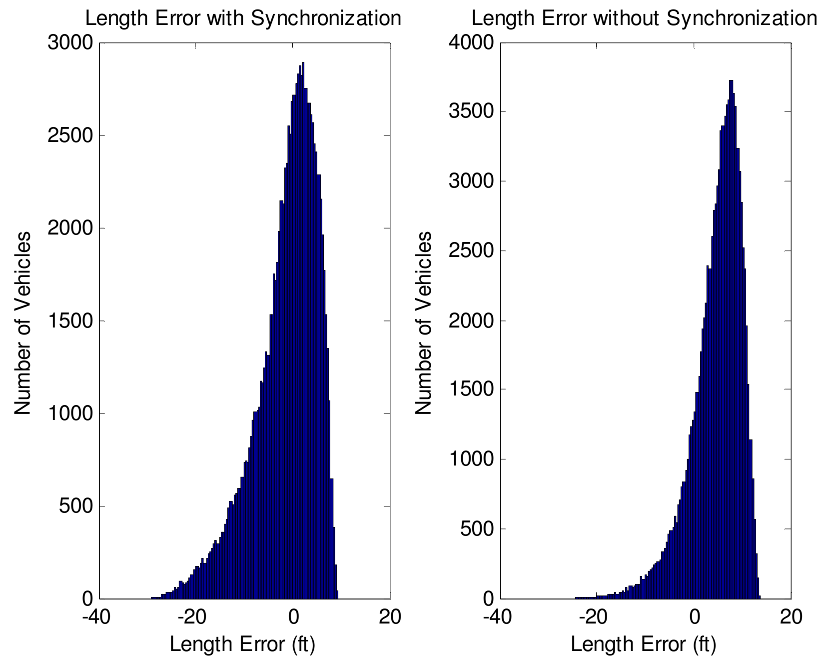

Figure 16: The effects of synchronous clocks on length error: with synchronization on the left and without on the right. Note that in this case the effective range is smaller and shifts to the right for the asynchronous data.

Table 1 shows summary statistics for these distributions when the distance between detectors is 4.6 feet for a vehicle traveling at 65 mph. In the appendix, fifth and ninety-fifth percentiles of speed and length errors for vehicles traveling past a detector with asynchronous and synchronous clocks are presented.

Table 1: The effects on synchronous clocks on length and speed errors

Length Error (ft)	With Synchronization	Without Synchronization		**Speed Error (mph)**	With Synchronization	Without Synchronization
Minimum	-28.98	-23.86		Minimum	-69.57	-63.02
Median	-0.02	5.78		Median	-0.04	13.4
Mean	-1.31	4.78		Mean	-3.32	10.93
Maximum	9.43	13.87		Maximum	22.12	32.75
Standard Deviation	6.42	5.07		Standard Deviation	16.07	12.51
Range	38.41	37.73		Range	91.69	95.77

Figure 17 and 18 below show the distribution of speed and length errors, respectively, for a detector operating at 40 Hz and 300 Hz, with the distance between the detectors of 4.6 feet (asynchronous clocks) and 20 feet (synchronous clocks). Figure 19 presents the cumulative distribution function for the speed and length errors of the same vehicles and detectors.

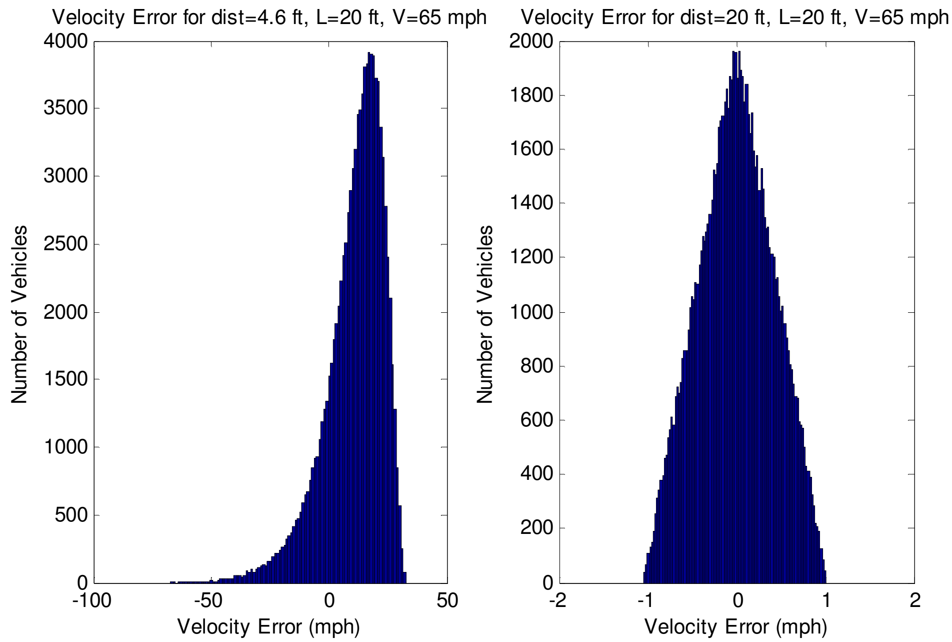

Figure 3: Histogram of speed error for 100,000 simulated vehicles over two detectors

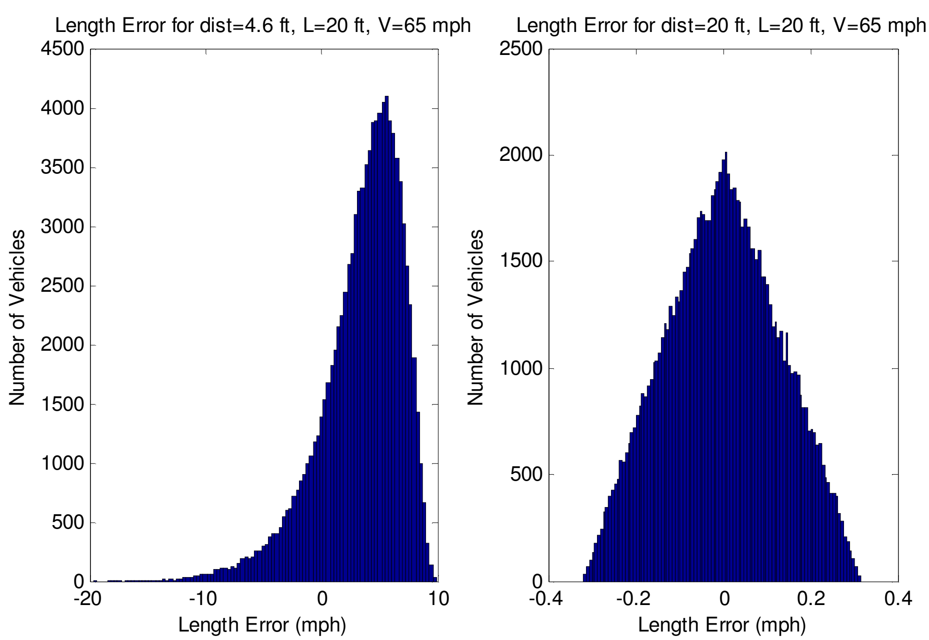

Figure 4: Histogram of length error for 100,000 simulated vehicles over two detectors

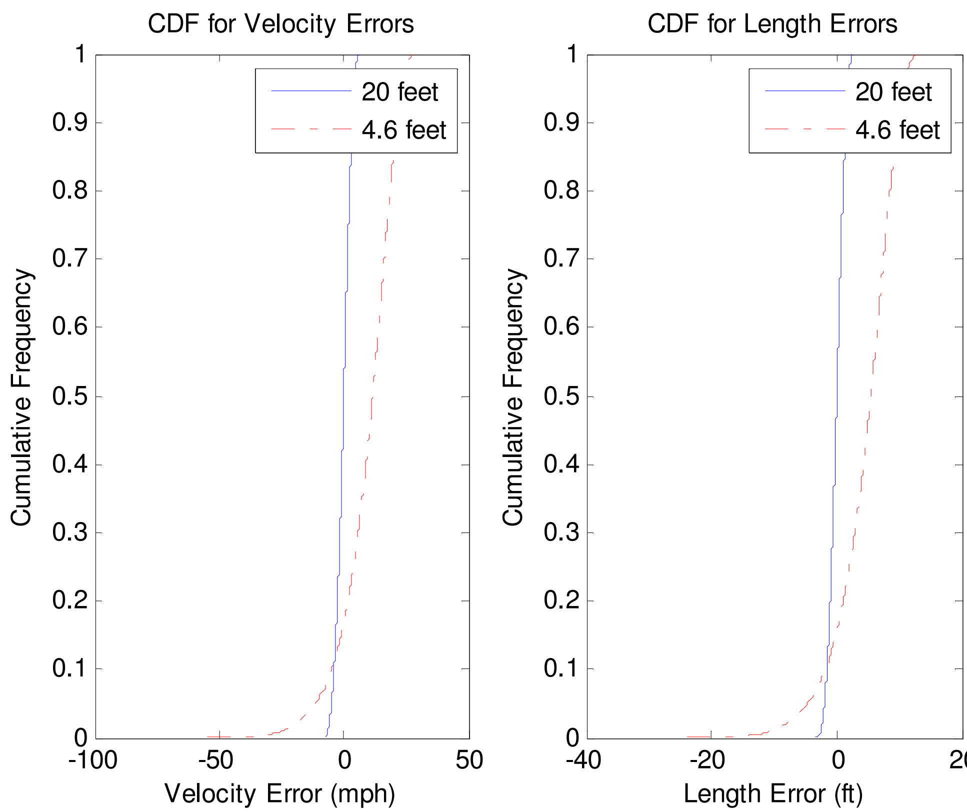

Figure 19: Cumulative distribution function for speed and length error

Dual loop detector station often exhibit drop-out errors when a vehicle is higher off from the ground, which is commonly seen in larger vehicles such as semi-trailer trucks. To eliminate the possible impacts of such drop-outs in the ground truth data, vehicles longer than 30 feet are excluded from this comparison. All of the speed measurement equations thus far assume acceleration is negligible, which is the case at free flow speeds. Because of these detector errors, only vehicles that have speeds between 55 and 90 mph and lengths between 12 and 30 feet are considered. Another difference arises due to the differing size of the detection zones. The loop detectors have approximately 6 foot long detection zones while the LIDAR detection zone is close to zero. The detection zone is included in the measured effective length, which will affect the data slightly due to the fact that the effective length is the length of the vehicle plus the length of the individual detection zone. The distribution between the LIDAR measured speeds and the loop detector measured speeds is shown in figure 20. The error was calculated by subtracting the loop detector speed from the LIDAR speed. Figure 21 shows the length error for the system. The length error was calculated by subtracting the loop detector effective length from the LIDAR length plus the 6 foot loop detection zone.

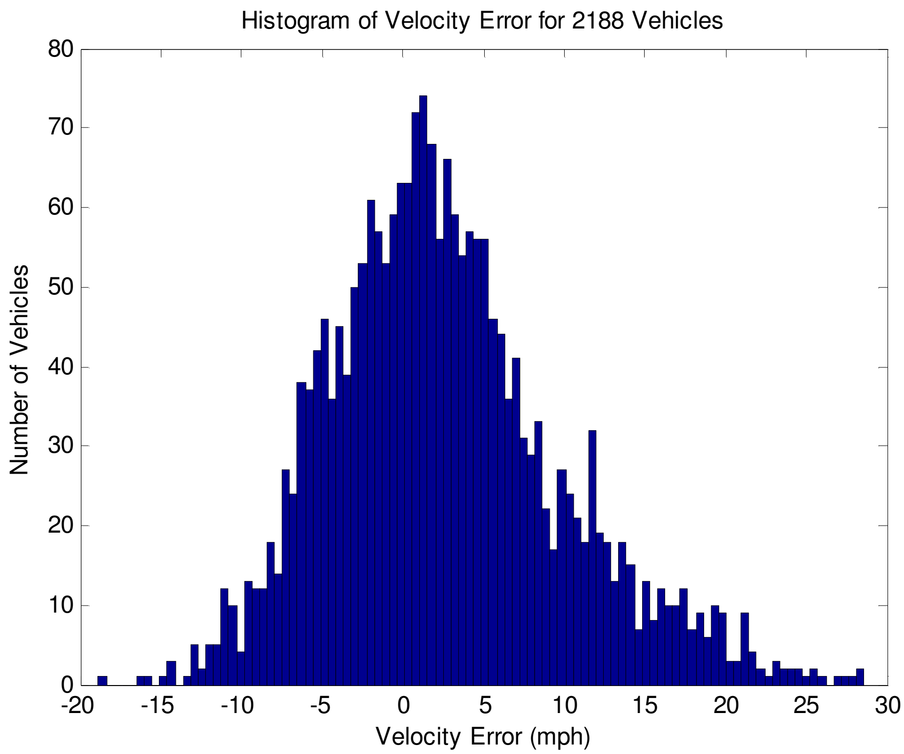

Figure 20: Histogram of speed error for vehicles at the classification station

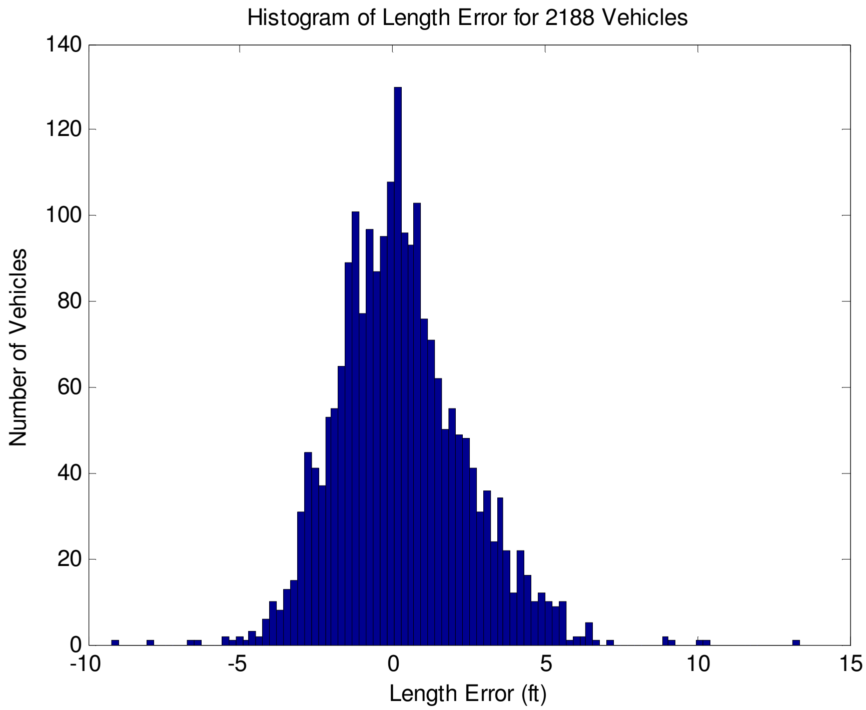

Figure 21: Histogram of speed error for vehicles at the classification station

The cumulative distribution plots in figure 22 and 23 use the measured distance between the LIDAR detectors of 4.6 feet, vehicle lengths of 28 feet, vehicle speeds of 65 mph, and sampling rate of 40 Hz. The predicted data is the possible distribution of each vehicle. Each vehicle tested 100 times each time generating a different pair of transition errors and yielding 100 measurements of speed and of length and the distribution was similar to the distribution seen in figure 18 above. The cumulative distribution function of the predicted should be similar to the actual error cumulative distribution, though some differences remain.

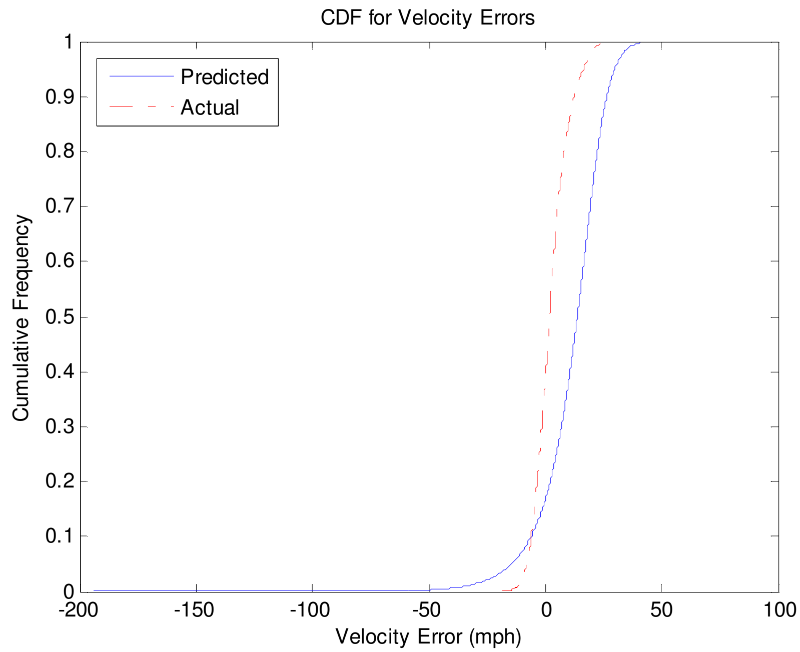

Figure 22: Cumulative distribution function of speed error for vehicles simulated and at the classification station

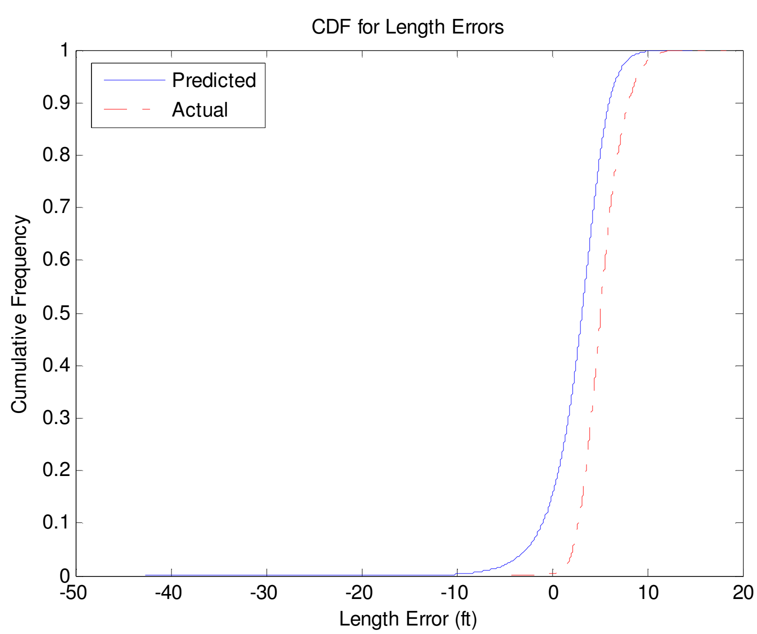

Figure 23: Cumulative distribution function of length error for vehicles simulated and at the classification station

Conclusions

This research has shown that the discretization impacts both speed and length measurements at a dual loop detector. However, at classification stations, the sampling frequency is large enough that the discretization errors are less than one foot for the cases studied in this work (e.g., Figure 7). Since the error is so small, few vehicles will be misclassified due to the length error. Although this work considered the lower frequency LIDAR contrasted against concurrent higher frequency classification station data for empirical validation, with the distance between detectors being different for LIDAR and the loop detectors, this work was not able be evaluate the two approaches evenly. Ultimately, it appears that although the classification station will exhibit some error due to the sampling rate, since the sampling rate is relatively high, the error will be relatively low. Finally, Figure 8 also shows results for 60 Hz data, which is common for traffic monitoring stations. This figure shows that free flow speed measurements may only be accurate to +/- 5 mph (the discretization error decreases at lower speeds because the ratio of one T to the net TT or OnT decreases).

Future Work

In order to properly determine if the sampling error is producing a large amount of error, the final classification data should be considered. The data is currently at 300 Hz and one possibility to avoid the detector spacing issue faced with the LIDAR is to down sample the data to 40 Hz. Once this is done, the distance between the loops will have no extra contribution and the error will only be due to the sampling rate.

References

[1] The Ohio Department of Transportation (2012) "Location and Design Manual, Volume 2". http://www.dot.state.oh.us/Divisions/Engineering/Hydraulic/LandD/Documents/Entire%20LandD_january%202012.pdf

[2] Grinstead, Charles; Snell, J. Laurie "Introduction to Probability". http://www.dartmouth.edu/~chance/teaching_aids/books_articles/probability_book/Chapter7.pdf

[3] Lee, H., Coifman, B., "Side-Fire LIDAR Based Vehicle Classification" *Transportation Research Record.* http://www2.ceegs.ohio-state.edu/~coifman/documents/LIDARclass.pdf

[4] Cassidy, M., Coifman, B., "Vehicle Reidentification and Travel Time Measurement on Congested Freeways", *Transportation Research: Part A,* 2002, vol 36, no 10, 2002, pp. 899-917. http://www2.ceegs.ohio-state.edu/~coifman/documents/VRI_basic.pdf

Appendix

Table 2 and 3 below demonstrate the fifth and ninety-fifth percentiles for speed and length errors of 100,000 simulated vehicles with distance between detectors of 20 feet. On the left the detector is operating at 300 Hz and on the right the detector is operating at 40 Hz, contrasting the difference between the loop detector (300 Hz) and the LIDAR (40 Hz). Only 5% of the speed and length error should fall below the fifth percentile or above the ninety-fifth percentile. The data at 40 Hz, it looks like the asynchronous sampling may actually reduce the range. A total of six conditions are evaluated, speeds at 80, 65, and 40 mph, and lengths at 28 and 46 feet. It can be seen that the length does not affect the speed error, but the speed affects the length error. The largest length error due to discretization occurs when the detector is operating at the lowest frequency and the longest vehicle passes at the highest speed.

Table 2: The fifth and ninety-fifth percentiles of simulated vehicles length and speed errors without synchronous clocks

Speed Error (mph) without Synchronization									
300 Hz		Speed (mph)			**40 Hz**		Speed (mph)		
Fifth Percentile		80	65	40	Fifth Percentile		80	65	40
Length (ft)	28	-2.32	-1.55	-0.57	Length (ft)	28	-20.86	-13.4	-4.7
	46	-2.31	-1.54	-0.57		46	-21.5	-13.39	-4.76
300 Hz		Speed (mph)			**40 Hz**		Speed (mph)		
Ninety-fifth Percentile		80	65	40	Ninety-fifth Percentile		80	65	40
Length (ft)	28	8.14	5.48	2.14	Length (ft)	28	36.79	26.56	11.92
	46	8.13	5.47	2.14		46	36.72	26.57	11.9

Speed Error (mph) with Synchronization									
300 Hz		Speed (mph)			**40 Hz**		Speed (mph)		
Fifth Percentile		80	65	40	Fifth Percentile		80	65	40
Length (ft)	28	-4.92	-3.23	-1.2	Length (ft)	28	-61.44	-35.61	-11.2
	46	-4.94	-3.23	-1.19		46	-61.1	-35.54	-11.17
300 Hz		Speed (mph)			**40 Hz**		Speed (mph)		
Ninety-fifth Percentile		80	65	40	Ninety-fifth Percentile		80	65	40
Length (ft)	28	4.37	2.94	1.12	Length (ft)	28	24.56	17.03	7.15
	46	4.4	2.94	1.13		46	24.31	16.93	7.14

Table 3: The fifth and ninety-fifth percentiles of simulated vehicles length and speed errors with synchronous clocks

Length Error (ft) without Synchronization									
300 Hz		Speed (mph)			**40 Hz**		Speed (mph)		
Fifth Percentile		80	65	40	Fifth Percentile		80	65	40
Length (ft)	28	-0.71	-0.58	-0.35	Length (ft)	28	-6.44	-5.05	-2.88
	46	-1.23	-1	-0.6		46	-11.25	-8.75	-5.04
300 Hz		Speed (mph)			**40 Hz**		Speed (mph)		
Ninety-fifth Percentile		80	65	40	Ninety-fifth Percentile		80	65	40
Length (ft)	28	2.76	2.29	1.45	Length (ft)	28	12.55	11.13	8.12
	46	4.58	3.8	2.42		46	20.73	18.46	13.44

Length Error (ft) with Synchronization									
300 Hz		Speed (mph)			**40 Hz**		Speed (mph)		
Fifth Percentile		80	65	40	Fifth Percentile		80	65	40
Length (ft)	28	-1.6	-1.28	-0.78	Length (ft)	28	-2.66	-2.13	-1.28
	46	-2.7	-2.17	-1.3		46	-4.31	-3.44	-2.05
300 Hz		Speed (mph)			**40 Hz**		Speed (mph)		
Ninety-fifth Percentile		80	65	40	Ninety-fifth Percentile		80	65	40
Length (ft)	28	1.42	1.17	0.73	Length (ft)	28	-19.89	-14.15	-7.24
	46	2.41	1.98	1.24		46	-33.47	-23.93	-12.24